ENDOPLASMIC FILAMENTS GENERATE THE MOTIVE FORCE FOR ROTATIONAL STREAMING IN *NITELLA*

NINA STRÖMGREN ALLEN

From the Department of Biological Sciences, State University of New York at Albany, Albany, New York 12222

ABSTRACT

The streaming endoplasm of characean cells has been shown to contain previously unreported endoplasmic filaments along which bending waves are observed under the light microscope using special techniques. The bending waves are similar to those propagated along sperm tails causing propulsion of sperm. In *Nitella* there is reason to believe that nearly all of the filaments are anchored in the cortex and that their beating propels the endoplasm in which they are suspended. This hypothesis is supported by calculations in which typical and average wave parameters have been inserted into the classical hydrodynamic equations derived for sperm tail bending waves. These calculations come within an order of magnitude of predicting the velocity of streaming and they show that waves of the character described, propagated along an estimated 52 m of endoplasmic filaments per cell, must generate a total motive force per cell within less than an order of magnitude of the forces measured experimentally by others. If we assume that undulating filaments produce the force driving the endoplasm, then the method described for measuring the motive force could lead to a lower than actual value for the motive force, since both centrifugation and vacuolar perfusion would reverse the orientation of some filaments. Observations of the initiation of particle translation in association with the filaments suggest that particle transport and wave propagation, which occur at the same velocity, may both be dependent on the same process. The possibility that some form of contractility provides the motive force for filament flection and particle transport is discussed.

INTRODUCTION

Rotational streaming in characean cells was discovered by Corti (8) nearly 200 yr ago and is perhaps the most remarkable example of cytoplasmic transport found in green plant cells, with streaming velocities observed of the order of 100 $\mu m\ s^{-1}$ (36 cm/h). Although the molecular mechanism of this movement is still far from clear, a great deal of new information has been discovered in recent years mainly due to technical advances. Work relevant to plant streaming before 1964 can be found in reviews by Kamiya (32, 33) and in Allen and Kamiya (4). Since then, studies on the ultrastructure of cells has revealed the presence of linear elements such as microtubules and microfilaments, which have been implicated in various cellular systems as responsible for motility. In one alga, *Caulerpa*, microtubules have been postulated to be related to cytoplasmic streaming (50). However, microfilaments have been strongly implicated to be involved in cytoplasmic streaming in

cells of both lower plants (41) and higher plants (42).

Streaming in most plant cells is sensitive to cytochalasin B and not to colchicine (62). For example, rotational streaming in *Nitella* is inhibited reversibly by $1-2 \times 10^{-5}$ M cytochalasin B (6, 37, 49, 64, and personal observation) after a delay of ca. 20 min. Although the microfilaments of the subcortical fibrils are not disrupted by cytochalasin B (6), this result may still implicate microfilaments in streaming in the material chosen for the present study.

Until recently only one report (61) of the presence of contractile proteins in *Nitella* existed. Palevitz et al. (43) have now reported the presence in *Nitella* extracts of microfilaments binding heavy meromyosin in characteristic arrowhead arrays that can be removed by ATP. These results are taken as evidence that actin is present in *Nitella*.

The internodal cell of *Nitella* is the ideal cell in which to search for a physical basis for the production of the motive force for cytoplasmic streaming. Other highly organized motile systems, such as muscle, flagella, mitotic spindles, etc., have all been shown to contain a system of organized linear elements which, in different ways, develop the motive force.

Internodal cells of *Nitella* are cylinders 2–5 cm long with a large central vacuole and a thin layer of cytoplasm lining the inside of the cell walls. Microtubules are found just inside the plasma membrane near the cell wall, not parallel to the direction of streaming generally, and not at the corticoendoplasmic interface (42, 46). Stationary chloroplasts are found embedded in the cortex in spiral rows. The endoplasm directly below the cortex moves as a giant twisted belt with the direction of the streaming parallel to the chloroplast rows. Many particles, including nuclei, are transported in the stream. Indifferent zones, where no streaming occurs, are located where the two opposing streams meet. Subcortical fibrils, running spirally parallel to the cell walls and chloroplast rows, as described by Kamitsubo (28, 29) are present in the shear zone between the cortex and the endoplasm. In the same position bundles of 50–100 microfilaments (50–70 Å in diameter) have been found by Nagai and Rebhun (41) in *Nitella*, and similar microfilaments were found in *Chara* by Pickett-Heaps (46). The currently accepted theory of rotational streaming is that the motive force is generated as an active shearing process at the interface between the cortical gel and the endoplasm (33, 34). At this interface there is a shear zone with an extremely sharp velocity gradient (ca. $100\ s^{-1}$). The active shearing theory was proposed to account for the observation that virtually the entire endoplasm streams as a belt at approximately the same velocity. Kamiya and Kuroda (34) also prepared endoplasm-filled cell fragments lacking a vacuole, in which the velocity was found to decrease from the cortex to the center of the cell. Damage inflicted in various ways to the cortex (17, 18, 32) was found to interfere with the generation of motive force. These results tend to support the localization of the motive force at the interface between the cortex and the endoplasm. The subcortical fibrils have been postulated as the generators of the motive force for streaming (28). Recently, Bradley (6) also obtained electron micrographs of similar microfilaments in *Nitella*, which show apparent cross-bridges between individual filaments in each bundle. Furthermore, he observed possible connections to endoplasmic reticulum and postulated that the endoplasmic reticulum might somehow act as a mechanical transducer effectively coupling the filaments and the streaming endoplasm.

Kamiya and Kuroda (35) confirmed Breckenheimer-Beyrich's (7) observation that the force of streaming could be balanced in one direction by centrifugal acceleration and developed the first method by which the motive force could be experimentally estimated. The values they obtained ($1-2$ dyn cm^{-2}) have since been confirmed from very similar results obtained by Tazawa (59) and Donaldson (9).

The first attempt to study the motility of isolated characean endoplasm was that of Yotsuyanagi (65, 66) who observed surface movements in isolated endoplasmic droplets caused by what later proved to be rotating polygonal fibrils. Jarosch (22) observed both rotating, circular and polygonal fibrils and undulating extended fibrils using dark-field microscopy. The fibrils were not always observable, but their presence could be deduced from the behavior of particles attached to them. Jarosch (22) also observed thickening and thinning of fibrils by lateral aggregation and disaggregation. Such thickening of fibrils has also been observed by Williamson (64) in endoplasmic droplets treated with cytochalasin B as streaming ceases.

Further studies on endoplasmic droplets have shown that polygonal fibrillar loops may propagate bending waves (i.e., the corners move) with or

without the transport of particles (23, 27, 28, 32, 38). Parts of the polygons have been demonstrated in electron micrographs to be composed of microfilaments (49).

It has been generally assumed following the active shearing theory of rotational streaming that the filaments active in isolated endoplasm bear some relationship to the generation of the motive force at the interface between the cortex and the endoplasm.

Jarosch (24) was the first to look for wave motion in the cortical and subcortical regions of *Nitellopsis* cells. He postulated that the rows of chloroplasts were waving with an amplitude of 0.5 μm as part of a force-producing oscillation. Further studies on endoplasmic droplets led Jarosch (25, 26) to postulate the presence of elastic helical fibrils which would rotate and generate the motive force by a screw-mechanical mechanism.

Kamitsubo (27, 28) first clearly demonstrated the presence of subcortical fibrils by light microscopy and showed that particles are propelled while in contact with these fibrils. Since the fibrils corresponded in location to the localization of the motive force according to the active shearing theory, it has been tacitly assumed that the generation of the motive force resides exclusively in these fibrils.

This assumption, while supported by a considerable body of information, does not preclude other possibilities. The present study attempts to delineate the characteristics of the undulations of endoplasmic filaments and of their fluid environment in order to determine whether filament undulation might provide the motive force for rotational streaming. One test of this question has been made by inserting measured wave parameters of endoplasmic filaments and measured endoplasmic viscosity values into classical hydrodynamic equations derived for flagellar undulation.

MATERIALS AND METHODS

Nitella Collection, Culture, and "Window Technique"

Nitella translucens (Pers.) Aug.,[1] collected from Loon Lake, N. Y., were cultivated in dechlorinated tap water over an inch of gravel in 15-gallon aquaria at ca. 27°C. In order to facilitate microscopic observation of the endoplasm of the large internodal cells, "windows" were made in the cortical layer of chloroplasts by a several minute exposure to a microbeam 100 μm in diameter illuminated by the visible light portion of the emission of a HBO-200 high-pressure mercury arc lamp (30, 31). Over a period of hours, the irradiated chloroplasts swell and are dislodged by the streaming endoplasm, leaving a window through which the interior of the cell can be viewed with exceptional clarity (Fig. 1). Isolated internodal cells were placed in Artificial Pond Water (consisting of 1 mM NaCl, 0.1 mM KCl, and 0.1 mM $CaCl_2$ per liter distilled water) in a growth chamber with a bank of four fluorescent lights at 24°C in a 12L:12D light cycle at least a day before the windows were made, and they were subsequently replaced in the chamber for several days to allow for recovery. For observation the *Nitella* window cells were placed between number 0 and number 1 cover slips in a special brass holder. The preparation was then sealed with melted Valap (vaseline, lanolin, and paraffin; 1:1:1) to prevent evaporation and consequent slight changes in focus during filming. As Kamitsubo (30) showed, the endoplasm first thickens and the subcortical fibrils disrupted by the window operation return within a few days so that observations can be made through a region of cortex lacking chloroplasts, but otherwise functionally intact. Internodal cells with or without windows survive for many weeks.

Microscopic Technique and Cinematography

Observations and photographic recording were performed with a Zeiss Photomicroscope II equipped with Nomarski differential interference attachments selected for very high contrasts (3). Using the 100× oil planachromatic objective paired with the aplanatic, achromatic condenser, the maximum extinction factor achieved was greater than 600 for a working aperture of ca. 0.95. Under these conditions, the depth of field for small particles is approximately 0.3 μm. Therefore it was possible to sample the endoplasm for the presence of filaments at specific levels within the endoplasm.

Cine records were made with an Arriflex camera at framing rates from 16 to 50 frames s^{-1} and with a LoCam camera at framing rates from 50 to 200 frames s^{-1} on Recordak film exposed for an ASA rating of 14 and processed in Diafine. For the highest possible contrast, a requirement for recording endoplasmic filaments, the 514-nm green line of a model 265 argon ion laser was used as a source in order that a very small bias compensation could be introduced to maximize interference contrast. The coherence of the raw laser beam is excessive for satisfactory image formation in the microscope; consequently the beam was phase randomized (39). It was necessary to use quite intense light (ca. 50 mW of power) to obtain the films, and such intensities might damage the cells and change the relative streaming

[1] Identified as *Nitella translucens* (Pers.) Ag. by Dr. Philip W. Cook, Department of Botany, University of Vermont, Burlington, Vt.

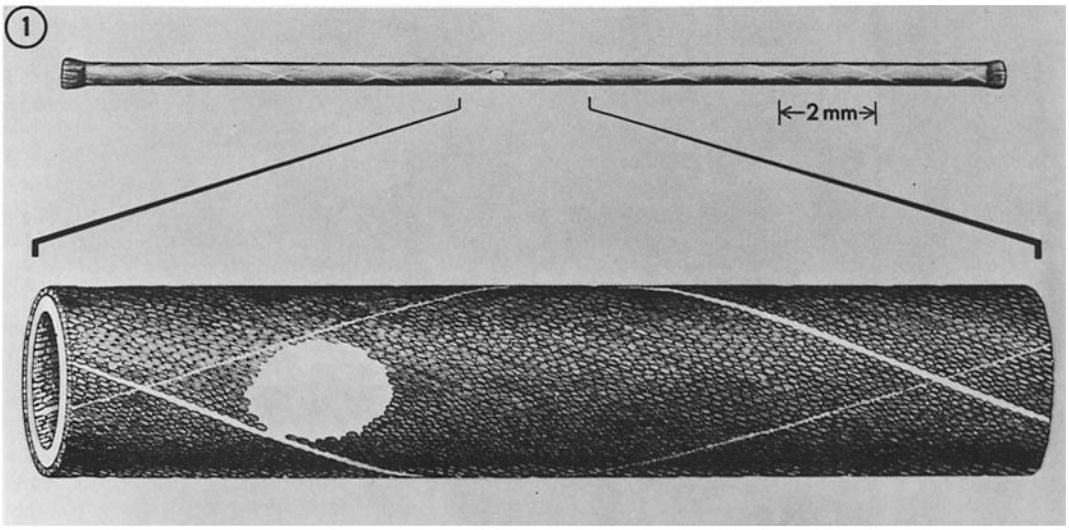

FIGURE 1 Drawing to scale of *N. translucens* internodal cell containing a cortical window as described by Kamitsubo (30). The upper drawing shows the entire cell. The lower drawing is an enlargement of the area containing the window. The rows of chloroplasts and the indifferent zones which lack chloroplasts wind spirally around the cell. The entire cytoplasm forms a continuous twisted belt.

rates (63). Therefore, care was taken not to illuminate cells except for short periods while filming.

Stroboscopic Illumination for Live Observation

For the observation of particles, the contrast requirements were far less demanding. Successful records were made on Ektachrome High Speed film (Eastman Kodak Co., Rochester, N. Y.) using a xenon source. The presence of endoplasmic filaments could be deduced from the configuration of particles passing through the field. Originally perceived[2] on projected films because of the stroboscopic character of the illumination, the observations could be made routinely on live material illuminated stroboscopically either by a sector wheel or by a Chadwick-Helmuth model 136 Strobex flash (Chadwick-Helmuth Co., Inc., Monrovia, Calif.) unit driven by an external signal generator at frequencies between 0 and 50 cycles s^{-1}.

Photographs of Stationary Filaments

For the demonstration of stationary filaments in quiescent cytoplasm, images of preselected optical sections were rapidly recorded on Panatomic-X film with the Zeiss photomicroscope and developed in Diafine.

[2] To observe the filament motions by the behavior of attached particles, it is necessary to fix the eye in the center of the screen (or field of view) so that the eye does not follow particles downstream. This method of observing is similar to the "flat eye" learned by students of Judo and Karate.

Cine Film Analysis

Analysis of particle motions was done with a Vanguard model M 16-C motion analyzer (Vanguard Motion Analyzers, Melville, Long Island, N.Y.). The positions of particles could be reproducibly localized along x and y coordinates to an accuracy of better than 0.3 μm.

Analysis of Brownian Motion of Endoplasmic Particles in Mechanically Stimulated Cells

Cytoplasmic streaming could be stopped temporarily by lightly tapping the cover glass.

To estimate the viscosity of *Nitella* endoplasm, 24 frames s^{-1} films of mechanically stimulated *Nitella* cell windows were analyzed in the Vanguard Motion Analyzer. Ten of the smallest particles (0.13–0.21 μm in radius) were tracked frame by frame until they passed out of focus. The total excursion X (in micrometers) was measured every 12 frames (0.5 s).

RESULTS

Observation and Perception of Undulating Filaments in Nitella Endoplasm

An untrained observer viewing the streaming of *Nitella* endoplasm either in vivo or on cine film normally sees only the passage of countless particles through the field at approximately uniform

velocity. The reason for this is that the untrained eye focuses on and follows particles moving downstream. If, however, the gaze is fixed in the center of the field, virtually all of the large particles (spherosomes, 34 and/or minivacuoles, 64) are perceived as moving through the field in serpentine sets. These sinusoidally undulating "strings of particles" were first noted while watching a film taken at 24 frames s^{-1} of optical sections of *N. translucens* endoplasm. Once this phenomenon has been observed, similar sets of particles can be seen undulating beneath the chloroplasts.

Stroboscopic flash illumination aids in the perception of the particle sets by multiplying their images. Enhancement of observations was observed at frequencies of ca. 24–36 s^{-1}.

In the initial experiments and films, only the serpentine sets of particles were seen, not the filaments themselves (1). The knowledge that isolated endoplasmic droplets contain fibrils that undulate and/or transport particles (23, 38, 64) suggested that the serpentine arrangement of particles could be explained by postulating their attachment to unseen filaments.

The Detection of Filaments in Streaming and Quiescent Endoplasm

The postulated filaments have not appeared in published electron micrographs of *Nitella* or *Chara* (for example, references 37, 41, 46). Our attempts to fix *Nitella* endoplasm for electron microscopy resulted in such poor preservation of the endoplasm that the presence of endoplasmic filaments could not be confirmed by electron microscopy. Our experience is similar to that of others who have attacked the same problem.

Cinematographic demonstration of a propagated bending wave along a poorly contrasted filament is complicated by the fact that, even framing at 100 s^{-1}, an exposure is $\frac{1}{200}$ s long. During that time, the ascending and descending portions of the wave are smeared over about 0.5 μm or at least twice the diameter of the thinnest resolvable filament. One would therefore expect to find short filament segments from the peaks and troughs of waves that are parallel to the direction of streaming. This expectation was confirmed.

It was necessary to take all possible measures to increase image contrast in order that the image of the waves, even though smeared by motion, would appear above the grain noise level of the film. These measures included the selection of cells with minimal light scattering and a number of measures for improving the extinction factor of the Nomarski differential interference contrast equipment with which the films were made. This approach has been successful, as can be seen in the final sequence of a published film (2). In any given optical section it is possible to see from 10 to 20 filaments not only during projection, but also on single projected frames.

The simplest way to demonstrate the entire endoplasmic filament complex is to stimulate the cell mechanically. This causes streaming to stop within 0.25 s. Streaming resumes after 1–2 min. During this interval optical sections were photographed at 1-μm increments starting at the cell wall and continuing through the cortex, shear zone, and endoplasm until the vacuole had been reached.

Filaments could be clearly seen in every optical section of the endoplasm (Figs. 2–7). In Fig. 2 the arrow indicates the direction of streaming. Some of the subcortical fibrils (ca. 0.2 μm in diameter) can be seen to branch. In Fig. 3, which is deeper in the endoplasm than Fig. 2, the arrow indicates branching points of thinner filaments. Fig. 4–6 demonstrate filaments present in sections successively closer to the vacuole. Fig. 7 is a section through the vacuole which appears in the center with endoplasmic ridges extending inward.

The Number of Filaments Present in a 100 μm^2 Cross Section of Endoplasm

The endoplasm of *Nitella* can vary in thickness from 5 to 30 μm. Cells grown under similar conditions show variability. 2-cm long cells with an endoplasm ca. 10 μm in thickness were used, if available.

The *Nitella* cell is cylindrical, hence any optical section will be at one level only in part of the field. The number of filaments present in areas 20 or 30 μm wide and 1 μm deep were counted in each optical section as seen with stroboscopic illumination.[3] Although the depth of focus was

[3] The 100× Nomarski system used in the study produced images with an optical thickness of about 0.3 μm. It has been shown (3) that particles essentially disappear from view when they have passed one particle diameter out of the field of view. For this reason, it was assumed that optical sections taken at 1-μm intervals would not record overlapping views of the same filament with a planar beat marked by particles approximately 1 μm in diameter.

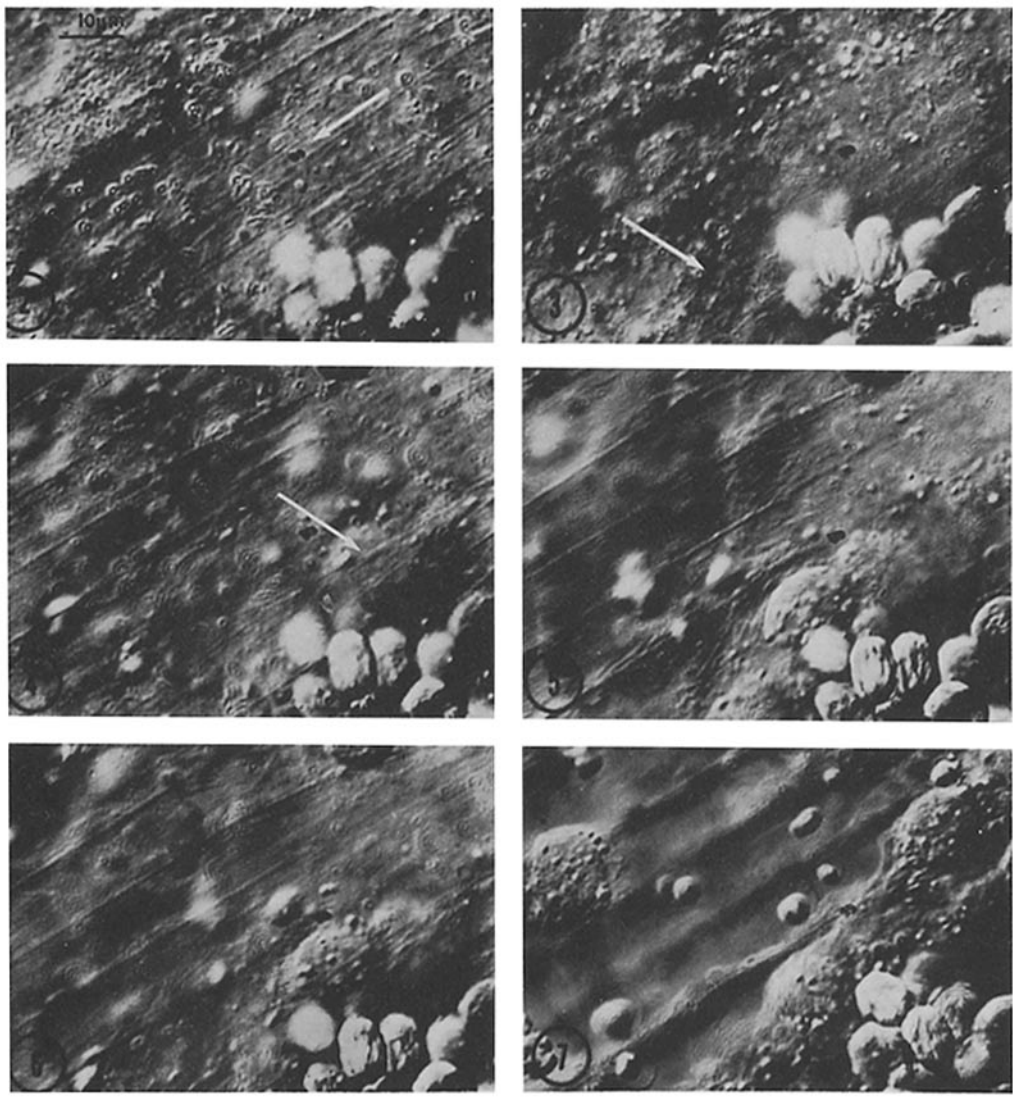

FIGURES 2–7 Endoplasmic filaments in quiescent endoplasm of *Nitella*. Endoplasmic filaments can be seen in all optical sections from the cortex to the vacuole Figs. (2–7). Mechanical stimulation was used to cause cessation of streaming so that the filaments could be observed and photographed. Note the branching of a fine filament from a larger straight filament as seen in Fig. 3 (arrow). Large arrow (Fig. 2) indicates the direction of streaming before stimulation and after resumption of streaming. Photographed on Panatomic X film with 100×, N.A. 1.3 planachromat objective, Nomarski differential interference optics. The 514 nm line of a 5-W argon ion laser was phase-randomized for illumination.

about 0.3 μm, it was found that a filament remained visible over 1 μm of vertical movement of the stage. It can be difficult to get a completely accurate count of the filaments, as they are moving rapidly and many are at the limit of detectability. 15 such estimates were made, and an average of 17 filaments/100 μm^2 was found with a minimum number of 10 filaments/100 μm^2 and a maximum of 24 filaments/100 μm^2.

Similarly, counts were made from photographs of filaments in optical sections such as those seen in Figs. 2–7. There an average of 16 filaments per 100 μm^2 was found.

Thus the estimate of the number of filaments may be a conservative one.

Mechanical Stimulation: Cessation and Resumption of Streaming

Comparable numbers of filaments were made directly visible by stopping cytoplasmic streaming (Figs. 2–7). It could be seen that as streaming resumed, particle motion began by transport along visible fibrils and filaments deep in the endoplasm. At first, particles traveled only short distances and appeared to be pulled forward to a new stopping point. Gradually, this jerky beginning, which one might call "saltation" (48–50), became more continuous and acquired the smooth character of cytoplasmic streaming. The form of movement seen during resumption is reminiscent of the jerky type of multistriate streaming observed in *Acetabularia* cells at velocities of 1–5 μm s^{-1}.

Frame-by-frame analysis showed that resumption of streaming is gradual in mechanically stimulated *Nitella* cells as was found by Sibaoka and Oda (53). The rate of streaming increases at first linearly with time and then approaches the normal streaming rate asymptotically.

Determination of the Viscosity of Nitella Endoplasm

To obtain viscosity values, the displacements of particles (in centimeters) were plotted and the root-mean-square displacements ($\bar{X}^2$) calculated and inserted into Einstein's equation (1905) corrected for two-dimensional analysis of the motion:

$$\eta = \frac{2kTt}{3\pi\bar{X}^2 r}$$

where: η = poise. 1 P = 100 cP (in a g cm^{-1} s^{-}). k = 1.385 × 10^{-16} erg deg^{-1} (Boltzmann's constant). T = absolute temperature (K). r = radius of the particle (cm). t = interval of time over which particle displacement is measured. π = 3.14159.

This analysis was carried out on film taken at 24 frames per s at 298°K.

An average value of 5.9 ± 2.26 cP was found for the viscosity of the endoplasm of *Nitella* cells in which streaming had been temporarily halted due to mechanical stimulation (Table I). Using the same method, Pekarek (45) found a value of 5 cP for the viscosity of the endoplasm of *Chara fragilis* at 22°C.

The Characteristics of Particle Transport and Wave Propagation Along Filaments

Observations and cine records on transport of particles on, and wave propagation by, filaments showed that both occurred at the velocity characteristic of the streaming of the entire cytoplasmic mass, with a measured average of 86.5 μm s^{-1}. Thus particles generally maintained a constant position with respect to each other and with respect to the crest of the wave and rode, like surfers, along the wave, but not necessarily along its crest. This can be seen in Fig. 8 depicting two out of 26 frames analyzed. In each successive frame, particles moved farther to the right. Occasionally a particle disappeared from one frame to the next, such as particle M which was lost in frame 2. If it had only gone out of focus, it was likely to reappear in later frames, but some particles appeared to have "fallen off" a filament, if they disappeared and did not reappear. The waves are transverse and vibrate in a plane parallel to the nearest tangent to the cell wall and cortex.

Fig. 9 is a sine wave generated from the data on wavelength and amplitude from the 26 successive

TABLE I

Summary of Data Used to Obtain the Viscosity of Nitella Endoplasm by Analysis of the Brownian Motion of Small Particles

Series no.	Radius of particle r (cm) (× 10^{-4})	Number of 0.5-s time intervals* measured	Root-mean-square displacement $\bar{X}^2$ (cm^2) (× 10^{-8})	η (centipoise)
1	0.18	3	0.31	7.8
2	0.17	5	0.47	5.5
3	0.17	5	0.51	5.2
4	0.21	5	0.97	2.1
5	0.16	6	0.60	4.6
6	0.15	6	0.47	6.2
7	0.18	8	0.35	6.9
8	0.13	4	0.30	11.1
9	0.18	5	0.55	4.4
10	0.18	3	0.46	5.3
			Average viscosity (η)	5.9‡

At a temperature of 298°K

* Each time interval is equal to 0.5 s or 12 frames in a 24 frame s^{-1} film.

‡ Standard deviation = ±2.26.

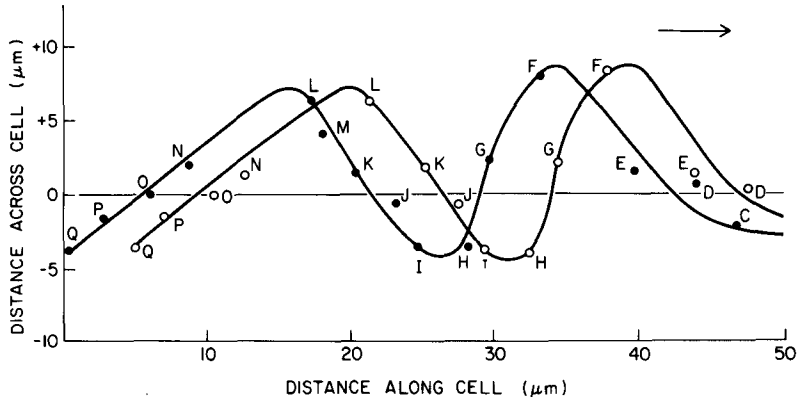

FIGURE 8 Sinusoidal bending waves along the endoplasmic filaments of *N. translucens*. Two successive positions of particles (closed circles, frame 1; open circles, frame 2) plotted in micrometers of a serpentine set of large refractile particles (spherosomes). The direction of streaming is indicated by the arrow in the upper right-hand corner and is made parallel to the x axis. Analysis was made from a film taken at 24 frames/s using/100× (N.A. 1.3) Nomarski differential interference contrast. Note that the particles maintain a constant spatial relationship to one another and more parallel to the filament axis at the same rate as the bend propagates.

frames. This sine curve could be superimposed on all the tracings of this wave which showed good, but not perfect, agreement. The filaments bend sinusoidally, but may not be sine waves in the strict sense. The motion of endoplasmic filaments is, if anything, more varied than that of sperm tail flagella, which do not undulate in true sine waves either (15).

Occasionally waves were seen to be perturbed (Fig. 10, arrow) as though mechanical interference had occurred. Such perturbations are seen at intervals of several seconds during live observation with stroboscopic light because of a greater sample size.

Table II summarizes the measured characteristics of the waves which varied over a wide range in wavelengths (17–144 μm) and amplitudes (2–7 μm). A typical wave (no. 3) had an average wavelength of 25 μm, amplitude equal to 5 μm, an average velocity of 88 μm s^{-1}, and therefore a frequency of 3.52 s^{-1}. The most noticeable waves were similar to this one, and it was much harder to find longer waves. The arithmetic averages for the first 16 waves listed in Table II were computed and show that these waves have a wavelength of 44 μm, an amplitude of 4.3 μm, and V_m equal to 86.5 μm s^{-1}.

The characteristics of the waves, listed in Table II, were obtained from more extensive plots of particle measurements like the one shown in Fig. 8

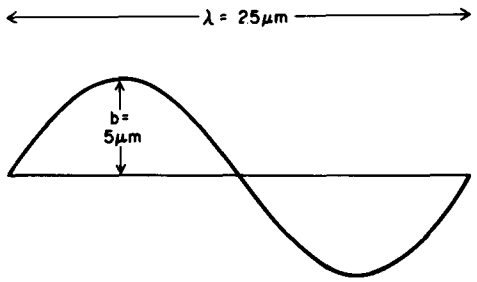

FIGURE 9 A mathematically generated sine wave with wavelength and amplitude averaged from extended measurements of the filament shown in Fig. 8.

of the 24 frame s^{-1} 100× film (2). All possible wavelengths and amplitudes were measured and averaged. Similarly, all the distances moved by the particles were measured and averaged to give particle velocities. Note that the particles characteristically travel in straight lines. Often slight variations in the velocities of particles in different serpentine particle sets were noted, so the velocities of all particles in the stream were not precisely the same.

The Number of Filaments Per Optical Section and the Total Length of Filaments Per Cell

The geometry of a *Nitella* cell is suitable for an analysis of the total number and length of fila-

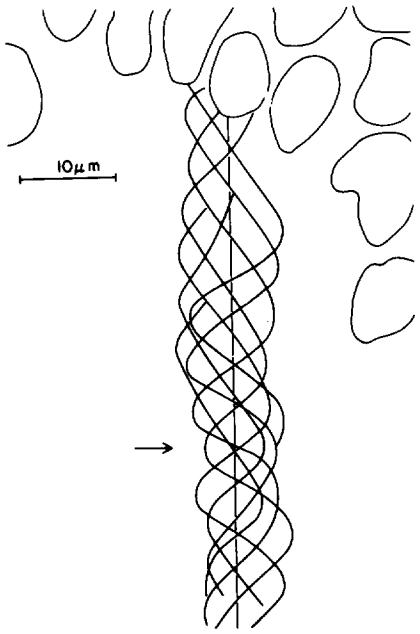

FIGURE 10 One endoplasmic filament observed through a cortical window in a *Nitella* cell traced in seven successive frames of a 24 frames/s film taken with a 100× objective (N.A. 1.3), Nomarksi differential interference contrast. The entire frame is 72 μm long. The large ellipsoids in the upper part of the trace represent the outlines of chloroplasts at the endge of the window. The endoplasmic filaments themselves were not visible, but their presence could be deduced from the positions of the particles used as markers. Note the occurrence of a perturbation in the wave form as it was propagated (arrow).

ments present in the endoplasm, since the cell can be considered to be a large cylinder of height h, and radius r. The endoplasm is a uniform layer just below the surface of the *Nitella* cell wall, and its surface area, volume, and cross-sectional area can be easily computed.

The cross-sectional area of the endoplasm (10 μm thick) in a cell with a radius of 250 μm and a length of 2.0 cm was found to be 15,000 μm^2. What was then the number of filaments in this cross-sectional area?

Optical sections at 1-μm intervals from the cortex through the endoplasm to the tonoplast revealed considerable numbers of filaments in every section, regardless of whether counts were made of the numbers of serpentine particle sets per 1-μm optical section (average of 17/100 μm^2) or the number of filaments visible per 1-μm optical section in quiescent cytoplasm (average of 16/100 μm^2). The thickness of endoplasm and the number of filaments will vary in different cells. A minimum of 12 and a maximum of 37 filaments/100 μm^2 have been counted.

By extrapolation, it was estimated that the total length of filaments in the 2-cm long internodal cell (this is the size of cell from which much of the data were generated) was about 5,234 cm or about 52 m. Using 25 μm as the approximate wavelength (for actively beating filaments), it was computed that 5,234 cm of undulating filaments corresponded to 2.1×10^6 wavelengths of filament.

DISCUSSION

The Geometry of the Subcortical Fibril-Endoplasmic Filament Complex in Nitella Cells

The system of subcortical fibrils discovered by Kamitsubo (27, 28) has now been shown to have ramifications which extend throughout the endoplasmic stream as depicted in the reconstruction in Fig. 11. The endoplasmic filaments are branches extending from the subcortical fibrils into the endoplasm. This branching is not immediately obvious to the observer because it occurs mostly in a plane perpendicular to the plane of optical sectioning so that the branches pass quickly out of focus. However, many photographs (e.g., Figs. 2–6) of serial optical sections revealed branch points, and it is suspected that many others went undetected because of the unfavorable angle of observation.

The branching of an endoplasmic filament leaving the subcortical plane of focus from a subcortical fibril can be seen also in a published photograph, Fig. II of Kamitsubo (30). Kamitsubo (29) has observed in vivo in centrifuged *Nitella* cells freely moving fibrillar loops, which he considered to be derived from the subcortical fibrils. In cine records polygonal fibrils appear that are similar to protoplasmic fibrils reported in endoplasmic droplets. Polygons have been shown in a few cases to be composed of microfilaments (37, 48). Williamson (64) reports that in freshly made endoplasmic droplets thin "strings of particles" are seen moving freely whereas in older or cytochalasin B-treated droplets the movement slows down and thicker fibrils are visible in such cells. Again, most highly motile fibrils are hard to perceive.

How Could Undulating Filaments Cause Streaming?

Sea urchin sperm move by flagellar undulation at velocities similar to the endoplasmic streaming velocity in *Nitella*. In swimming forward, sperm react against their fluid environment, the viscosity of which is known, setting part of it in motion in the opposite direction. If, in the mind's eye, one constructed a model system consisting of a glass capillary with the heads of thousands of sperm anchored at the capillary wall with the tails pointed down the capillary in the same direction, it is intuitively obvious that the beating of the sperm tails would cause fluid to flow down the capillary. This type of fluid propulsion system is found in sponges in which the flagellated choanocytes provide the force for fluid flow.

TABLE II

Averaged Values Characterizing Waves of the Undulating Filaments

Wave no.	λ	b	V_m (μm)/(s^{-1})	$f = \frac{V_m}{\lambda}$ (s^{-1})
	μm	μm		
1	17	2.0	85	5.0
2	22	5.0	88	4.0
3	25	5.0	88	3.5
4	25	4.0	86	3.4
5	25	5.1	76	3.0
6	36	4.0	97	2.7
7	36	3.5	92	2.6
8	37	5.5	84	2.3
9	43	4.0	86	2.0
10	44	4.4	70	1.6
11	48	4.8	95	2.0
12	56	3.3	96	1.7
13	62	4.1	99	1.6
14	64	4.6	95	1.5
15	65	7.0	70	1.1
16	100	3.0	77	0.76
17*	144	2.2	82	0.56
Average of waves 1–16	44.1	4.3		
	Arithmetic mean		86.5	1.96

λ is wavelength, b is amplitude, V_m is measured particle velocity, and f is the frequency of the waves.

* Wave 17 had such a long wavelength that one had to estimate its length (recall that the field width is equal to 72 μm). 17 has therefore been left out of the average wave calculations.

Although the geometry of the *Nitella* internodal cell is somewhat more complex than the capillary model, it is intuitively plausible that endoplasmic filaments undulating like flagella could produce rotational streaming by their combined action. To determine whether it is possible that they do cause streaming, it is necessary to know the characteristics of the undulation and to have a reasonably accurate estimate of the total number and length of filaments. With this information it is possible to apply as a first approximation the classical hydrodynamic equations of Taylor (57, 58) and Gray and Hancock (15) derived for sperm propulsion to estimate both the expected velocity of streaming and the motive force that observed undulations must generate.

The suggestion that unseen undulating filaments could cause streaming is not new (cf. Jarosch [24], Taylor [56], Thornburg [60], Hejnowicz [19], MacRobbie [40], and Fensom [13]). Although many workers have probably considered this possibility, the present report seems to be the first evidence to support it.

Gray and Hancock (15) derived equations that predicted the velocity of either an intact or a headless sperm from the frequency, amplitude, and wavelength of their undulations (Table III). Eq. a, Table III, was derived to yield the velocity of a sperm with a head, which of course would slow down the velocity of the sperm. The third term of Eq. a has a correction factor for the head of the sperm. Eq. b, Table III, was derived to yield the velocity of headless filaments with waves of relatively large amplitude.

As Gray (14) stated in his monograph on cilia: "Any real conception of ciliary movement must eventually rest on a proper understanding of the hydrodynamic problems which are involved." The same could be said for the conception of the function of the filaments in *Nitella*, where we have insufficient information regarding the rheological nature of the endoplasm. It is still valuable to make some first-order approximations for the expected force and velocity based on the assumption that filament undulation generates the motive force.

In the case of *Nitella* endoplasmic filaments, the wave characteristics inserted into the equation for a headless flagellum (Table III, Eq. b) predict velocities within a factor of three of the observed

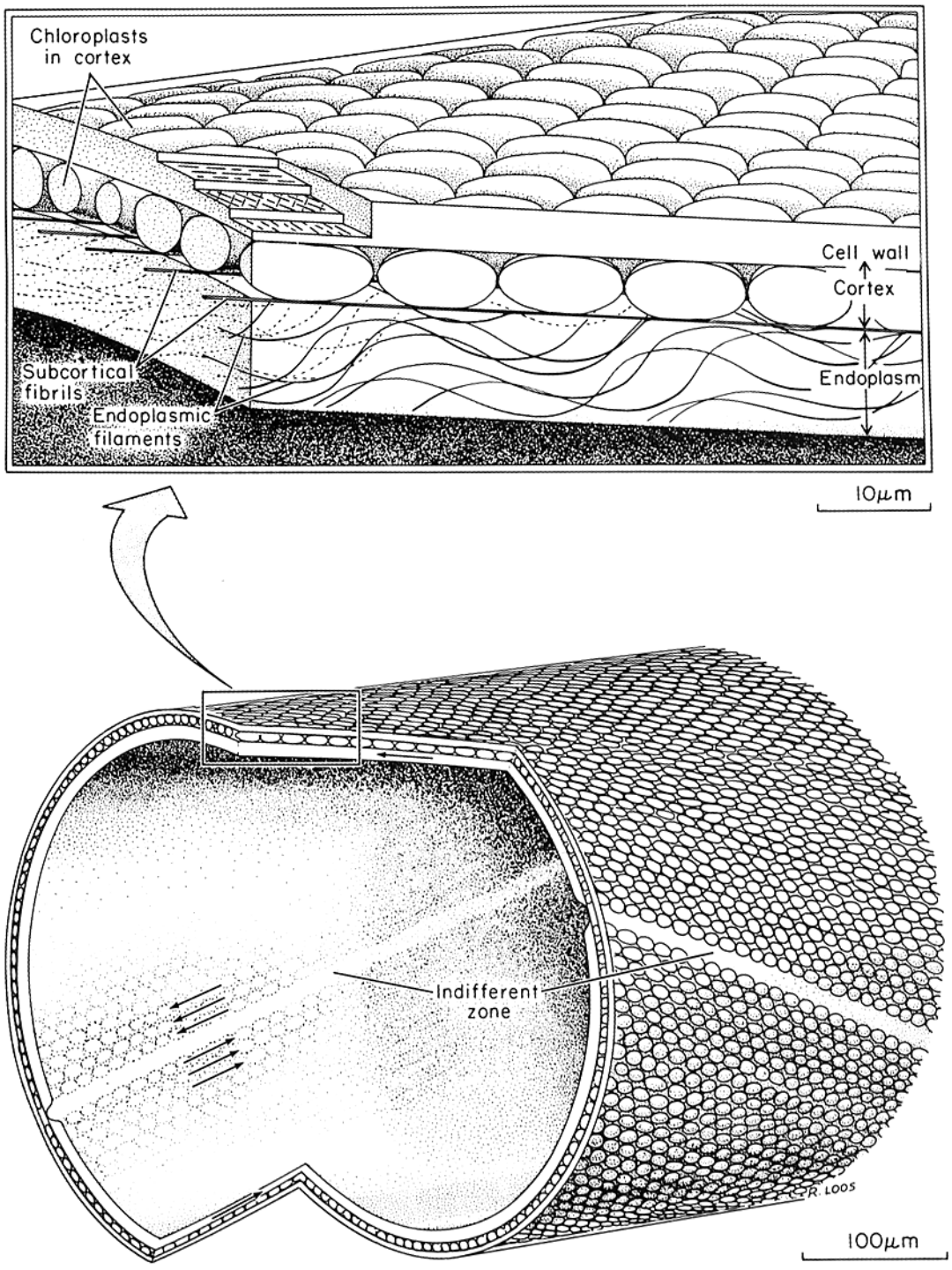

FIGURE 11 Top. Diagram illustrating the spatial relationships of the endoplasmic filaments with respect to the cortex, subcortical fibrils, and endoplasm, as reconstructed from optical sections of *Nitella* cells. Below. Diagram showing the relationship of the top diagram to the whole cell. Note that the cell is cut partly in cross section, partly in skewed sagittal section following the direction of the chloroplast rows. Drawn from a scale model.

TABLE III

Comparison of Nitella Filaments with Sea Urchin Flagella

		Sea urchin sperm flagella	*Nitella* filaments
(b)	amplitude of waves	4 μm	5 μm
(λ)	wavelength	24 μm	25 μm
(n)	number of simultaneous waves	1.3	$> 10 < \infty$
(f)	frequency of waves	35 s^{-1}	3.52 s^{-1}
(a)	radius of head	0.5 μm	—
(d)	radius of tail	0.2 μm	approx. 0.1 μm
(V_m)	mean observed velocity	191.4 μm s^{-1}	88 μm s^{-1}
(V_c)	calculated velocity	191 μm s^{-1} *	27 μm s^{-1} ‡

$$* V_c = \left(\frac{2f\pi^2b^2}{\lambda}\right)\left\{\left[\frac{1}{1+(4\pi^2b^2/\lambda^2)}\right] - \left(\frac{1}{[1+(2\pi^2b^2/\lambda^2)]^{1/2}\,(3a/n\lambda)([\log d/2\lambda]+1)}\right)\right\} \quad \text{(a)}$$

$$‡ V_c = \left(\frac{2f\pi^2b^2}{\lambda}\right)\left[\frac{1}{1+(4\pi^2b^2/\lambda^2)}\right] \quad \text{(b)}$$

Eqs. a and b are Eqs. XXVI and XXI, respectively, from Gray and Hancock (15).

value (Table III). This should be regarded as quite a satisfactory agreement when it is considered, for example, that the filaments might act cooperatively to product a larger velocity than predicted.

The discrepancy between the observed and calculated streaming values might also result from the fact that the cytoplasm is highly non-Newtonian and structurally anisotropic[4] while the equations were derived for flagellar motion in a Newtonian fluid.[5] *Nitella* endoplasm has a low apparent *micro*viscosity (6 cP) as determined by the Brownian motion method. However, forcing endoplasm of an isolated cytoplast to flow through an agar capillary produces apparent *macro*viscosity values at low rates of shear in the range of 250 cP (36). This discrepancy between macro- and microviscosity values suggests the presence of weakly cross-linked elements. According to Donaldson (9, p. 331) the best fit for Kamiya and Kuroda's (35) rheological data gives η = 145 cP at low rates of shear with a much lower probable *in situ* viscosity. In the derivation of the hydrodynamic equations, viscosity enters both as a drag force and as a factor analogous to traction. When a flagellum beats, it "pushes against" the viscosity of the medium. If the "traction viscosity" were similar to the macroviscosity and the "drag viscosity" similar to the microviscosity, the discrepancy between observed and calculated values would be explained.

The very incomplete data available on the rheological properties of *Nitella* endoplasm suggest the possibility that the viscous drag around the filaments may be approximated by the microviscosity of ca. 6 cP, while the traction viscosity against which the filament beats may be closer to the macroviscosity of 250 cP. Such a difference in viscous properties in drag and propulsion could easily account for a discrepancy of a factor of 3 in the observed and predicted velocities.

The Motive Force Generated by Undulating Filaments

As is well known, the rates of cytoplasmic streaming and of ciliary and flagellar motion depend on two factors, the viscosity of the fluid and the motive force. Large bodies, such as dolphins, have a high Reynolds number, which means that when they propel themselves in water, they make use of inertia in the surrounding fluid. Microscopic bodies have very small Reynolds numbers (an amoeba would have a Reynolds number on the order of 10^{-3} or less) and therefore when being propelled the stresses due to viscosity may be many thousands of times as great as those due to inertia. This concept also implies that if the

[4] Anisotropic by virtue of the presence of linear elements parallel to the direction of streaming.

[5] Newtonian fluids have a linear force-flow relation and a viscosity independent of the rate of shear.

force propelling a microscopic object is removed, the object will immediately come to a halt, since the inertial forces are negligible. Taylor (57, 58) employed these and other hydrodynamic considerations to derive equations for sperm tails with which one can compute the rate at which energy must be supplied to maintain the waves against the reaction of the surrounding fluid. Similarly, the propulsive and resistive forces per wavelength generated by a propagated bending wave along an endoplasmic filament can be computed employing the hydrodynamic considerations of Taylor (57, 58), Hancock (16), and Gray and Hancock (15). The original equations of Taylor predicting the velocity of sperm were derived for a filament infinitely long along which planar, transverse waves are propagated. Hancock (16) demonstrated that the results of calculations for a finite filament are very near those of an infinite filament with the same wave motion. The endoplasmic filament length is unknown, but at least two wavelengths were averaged in the data used here. Gray and Hancock (15) derived simpler equations for both the V_c (Eq. b, Table III) and the propulsive force. In calculating the propulsive force the surface coefficients of resistance C_N and C_T are, respectively, acting normal and parallel to the axis of a thin cylinder. Thus the propulsive force (F_p) per wavelength is:

$$F_p = \frac{2\pi^2 b^2 V_m (C_N - C_T)}{\lambda} \qquad (1)$$

where b is the amplitude, V_m the measured velocity, λ the wavelength, and C_N and C_T are calculated from the equation

$$C_T = \frac{-2\pi\eta}{0.5 + (\ln r/\lambda)} \qquad (2)$$

where η is the viscosity and r the radius of the flagellum. It was shown by Hancock (16) that for very thin filaments

$$C_N = 2\ C_T \qquad (3)$$

which was of importance, since the equations could be derived, then, for waves with relatively large amplitude. The resistive force (F_R) is

$$F_R = C_T\ \lambda\ V_m \qquad (4)$$

where V_m is the measured velocity and λ is the wavelength.

As can be seen in the sample calculations in Table IV, if one used the above equations, a typical "active wave" with a wavelength 25 μm, amplitude 5 μm, V_m of 88 μm s^{-1} and frequency equal to 3.52 s^{-1} develops a propulsive force of 1.39×10^{-6} dyn per wavelength and a resistive force equal to 1.76×10^{-6} dyn per wavelength using the measured value of 6×10^{-2} P for the viscosity. According to Newton's Third Law the F_P should equal the F_R; clearly the agreement is quite good.

The same calculations were carried out for all the waves measured (listed by wavelength) and the results are summarized in Table V. At longer wavelengths a smaller propulsive force is produced. As the waves get longer a discrepancy appears between the F_P and the F_R. The reason for choosing a wave around 25 μm as the example for calculations was that (*a*) most of the waves seen were of this magnitude and (*b*) from the F_P calculations it can be seen that the waves with a long wavelength contributed much less propulsive force. It was for this reason that only "actively waving" filaments were counted in the estimate of 17 filaments per μm^2 of endoplasm. Table V also includes the V_C, the velocity calculated for each wave, using the equations described earlier. As the calculated force produced by a wave decreases, so does the calculated velocity. Measured velocities show no such drop at longer wavelengths. In this system the invariant quantity is the velocity of wave propagation, and the frequency is derived from velocity/wavelength. In light waves, a more familiar system, it is the frequency that is invariant, and the velocity and wavelength are dependent variables as the light waves enter media of different refractive index. In *Nitella* we can observe only a few wavelengths of each filament, and it is a possibility that there are changes in amplitude along the total length of a filament. Similarly, in sperm tails the undulations are not perfect sine waves and the amplitude varies from head to tip. In any undulating filament, the amplitude of a wave depends not only on the force distorting the filament, but also on the stiffness and diameter of the structure. In a filament composed of microfilaments it would not be surprising if the amplitude varied inversely with diameter. There is some evidence that this may be the case, but it is not possible to test rigorously since the diameter of the filaments is near the limit of resolution of the microscope.

The typical 2-cm-long internodal cell referred to

TABLE IV

Calculation of the Propulsive Force and Resistive Force Per Wavelength of an Endoplasmic Filament with $\lambda = 25\ \mu m$, $b = 5\ \mu m$, $V_m = 88\ \mu m\ s^{-1}$, and $f = 3.52\ s^{-1}$

Calculation of propulsive force:

$$F_P = \frac{2\pi^2 b^2 V_m (C_N - C_T)}{\lambda}$$

$$F_P = \frac{2\pi^2(25 \times 10^{-8}\ cm^2)(88 \times 10^{-4}\ cm\ s^{-1})(8 \times 10^{-2}\ g\ cm^{-1}\ s^{-1})}{25 \times 10^{-4}\ cm}$$

$$F_P = 1.39 \times 10^{-6}\ dyn\ \lambda^{-1}$$

Calculation of resistive force:

$$F_R = C_T\ \lambda\ V_m$$

$$F_R = (8 \times 10^{-2}\ g\ cm^{-1}\ s^{-1})(25 \times 10^{-4}\ cm)(88 \times 10^{-4}\ cm\ s^{-1})$$

$$F_R = 1.76 \times 10^{-6}\ dyn\ \lambda^{-1}$$

Calculation of C_T and C_N:

$$C_T = -\frac{2\pi\eta\ (poise)}{0.5 + \ln(r/\lambda)}$$

$$C_T = -\frac{2\pi\ (6 \times 10^{-2}\ P)}{0.5 + \ln[(1.0 \times 10^{-5}\ cm)/(25 \times 10^{-4}\ cm)]}$$

$$C_T = 0.08\ g\ cm^{-1}\ s^{-1}$$

Since $C_N = 2\ C_T$

Then $C_N = 2\ (0.08)$

$$C_N = 0.16\ g\ cm^{-1}\ s^{-1}$$

The value used for viscosity (η) was the one measured as shown in Table I, i.e., $= 6 \times 10^{-2}$ P.

earlier was shown to have 5,234 cm of filaments. As already mentioned, wave no. 3 (Table V) thus has 2.1×10^6 wavelengths of total filament. The mean force of wave no. 3 was calculated to be 1.39×10^{-6} dyn λ^{-1}; thus the force developed by the sum total of the waves amounts to ca. 2.92 dyn ([1.39×10^{-6} dyn λ^{-1}][2.1×10^6 number of waves]). For the endoplasmic filaments to apply this force to the streaming endoplasm, they must be anchored in the cortex, which has an area of ca. 0.3141 cm^2. Thus the force developed by the total endoplasmic filament per square centimeter of cortex can be computed to be *9.3 dyn cm^{-2}*. This calculation assumes filaments with a wavelength of 25 μm and an amplitude of 5 μm. Not all the waves are like this "typical active" wave. The force per area of the average wave 1–16 (Tabel V) was similarly calculated to be 9.9 dyn cm^{-2}. Thus the results of force calculations for the active wave and the "average wave" are essentially the same.

It is interesting that the above calculated values are close to those measured for the motive force by two methods used by different groups of investigators. Thus the motive force measured by Kamiya and Kuroda (35) was in a range of 1–2 dyn cm^{-2} using the centrifuge "balance-acceleration" method; whereas Tazawa (59) and Donaldson (9) using the vacuolar perfusion method measured the motive force as 1.4–2.0 dyn cm^{-2} and 3.6 dyn cm^{-2}, respectively. All of these motive force

TABLE V

The Calculated Values for Propulsive Force (F_P), Resistive Force (F_R), and Velocity (V_C) for All Waves that were Measured

Wave no.	Wavelength (λ)	C_T	C_N	F_P	F_R	V calculated*	V calculated‡
	μm			$dyn\ \lambda^{-1}$	$dyn\ \lambda^{-1}$	$\mu m\ cm^{-2}$	$\mu m\ cm^{-2}$
1	17	0.08	0.16	3.08×10^{-7}	1.16×10^{-6}	15	23
2	22	0.08	0.16	1.56×10^{-6}	1.54×10^{-6}	30	89
3	25	0.08	0.16	1.39×10^{-6}	1.76×10^{-6}	27	69
4	25	0.08	0.16	8.68×10^{-7}	1.72×10^{-6}	21	43
5	25	0.08	0.16	1.24×10^{-6}	1.52×10^{-6}	23	62
6	36	0.07	0.14	5.96×10^{-7}	2.44×10^{-6}	16	24
7	36	0.07	0.14	4.32×10^{-7}	2.4×10^{-6}	13	18
8	37	0.07	0.14	9.6×10^{-7}	2.2×10^{-6}	20	37
9	43	0.07	0.14	4.3×10^{-7}	2.4×10^{-6}	11	15
10	44	0.07	0.14	4.12×10^{-7}	2.0×10^{-6}	10	14
11	48	0.066	0.12	5.92×10^{-7}	3.0×10^{-6}	14	19
12	56	0.064	0.12	2.22×10^{-7}	3.2×10^{-6}	6	7
13	62	0.064	0.12	3.18×10^{-7}	3.6×10^{-6}	7	9
14	64	0.062	0.12	3.84×10^{-7}	3.8×10^{-6}	8	10
15	65	0.060	0.12	6.24×10^{-7}	2.8×10^{-6}	11	17
16	100	0.058	0.12	7.94×10^{-8}	4.4×10^{-6}	1	1
17	144	0.056	0.11	3.0×10^{-8}	6.6×10^{-6}	0.4	0.4
Average 1–16	44.1	0.070	0.14	2.6×10^{-6}	12.2×10^{-6}	14	27

* $V_C = \frac{2f\pi^2b^2}{\lambda} \left[\frac{1}{1 + (4\pi^2b^2/\lambda^2)}\right]$

‡ $V_C = \frac{2f\pi^2b^2}{\lambda}$

measurements were made under the assumption that the motive force was generated at the shear zone, the boundary between cortex and endoplasm. The counter force (centrifugation or counterflow through the centrol vacuole) probably would disturb the pattern of movement of the endoplasmic filaments, possibly reducing the measured motive force somewhat.

Some Speculations Regarding the Mechanisms of Undulation and Particle Transport

It is now established that the subcortical fibrils and endoplasmic filaments can do two things: transport particles and propagate undulations. If anchored along their entire length, as are the subcortical fibrils, no undulations are observed, contrary to the already mentioned report of Jarosch (24). Fibrils and filaments that are free in the endoplasm, do, however, undulate as well as transport particles.

There are indications from recent studies on sea urchin sperm flagella that axonemal filaments normally exhibit bending waves due to active sliding between microtubule pairs (52, 54), probably by virtue of limited sliding activity of the dynein arms between microtubular pairs. Under in vivo conditions it is probable that the sliding is quite restricted, but on gentle digestion with trypsin, which removes the membrane around the axonemes and some of the protein cross-linking the microtubules, active sliding causes a telescopic sliding of microtubular pairs relative to one another.

It is interesting to note that flagella also have the capacity to cause transport apparently by the same kind of limited active shear that produces bending. The flagella of *Peranema* and *Chlamydomonas*,[6] for example, can actively slide along glass surfaces even when not propagating bending waves. Holwill

[6] Robert Day Allen, personal communication.

and Sleigh (20) found that *Ochromonas malhemensis* had currents of water flowing about the flagellum, when temporarily attached to the substrate. Douglas and Holwill (11) also have observed that extracted short flagella from *Crithidia oncopelti* can propagate bends when one end of an organelle becomes attached to a surface.

Almost certainly the system of subcortical fibrils and endoplasmic filaments is not composed of microtubules because streaming in *Nitella* is inhibited by cytochalasin B, not by colchicine. The results of Nagai and Rebhun (41) established that microfilaments are the linear elements of which the subcortical fibrils are composed. The findings of Barry (5) suggested similar ionic requirements for excitation-streaming coupling as for excitation-contraction coupling for muscle. This evidence is indirect. As mentioned (43), *Nitella* contains at least the actin part of the actin-myosin system present not only in muscle, amoebae (55), many animal cells, and slime molds. If actin (and myosin) are present, then we are already conditioned by the elegant experiments of Huxley (21) to expect active sliding as in striated and probably smooth muscle as well (51).

I am very grateful to Dr. John Terborgh, who as my thesis advisor encouraged and supported the early phases of the present study, and to Dr. Robert Day Allen for valuable discussions of the work and careful reading of the manuscript. I also would like to thank Dr. Eiji Kamitsubo for his advice on how to prepare "windows" in internodal cells, and to Dr. Robert Rikmenspoel for the use of his Vanguard Motion Analyzer and High-Speed Camera. Dr. Robert Rikmenspoel, Dr. Angelo Skalafuris, and Dr. Harry Frisch were all very helpful in discussions regarding the hydrodynamic concepts used in the study. I also wish to thank Alice Jacklet, Ryland Loos, Robert Speck, Marcia Cockrell, Dale Rice, and Robert Zeh for various kinds of specialized technical assistance.

This work was supported in part by the National Institutes of Health Predoctoral Fellowship (no. 5-FO1 GM-38,386) at the University of Maryland and in part by Research Grant GM 18854 from the National Institute of General Medical Science administered by Dr. Robert D. Allen.

Received for publication 26 October 1973, and in revised form 18 April 1974.

REFERENCES

1. ALLEN, N. S. 1973. Endoplasmic filaments generate the motive force for rotational streaming in *Nitella*. Doctoral Thesis. University of Maryland, College Park, Md.
2. ALLEN, N. S. 1973. Endoplasmic filaments in *Nitella translucens*. Film. Calvin Communications, Inc., Kansas City, Mo.
3. ALLEN, R. D., G. B. DAVID, and G. NOMARSKI. 1969. The Zeiss-Nomarski differential interference equipment for transmitted-light microscopy. *Arch. Wiss. Mikrosk. Mikrosk. Tech.* **69**:193.
4. ALLEN, R. D., and N. KAMIYA, editors. 1964. Primitive motile systems in cell biology. Academic Press, Inc., New York. 1–642.
5. BARRY, W. H. 1968. Coupling of excitation and cessation of cyclosis in *Nitella:* role of divalent cations. *J. Cell. Physiol.* **72**:153.
6. BRADLEY, M. O. 1973. Microfilaments and cytoplasmic streaming: inhibition of streaming with cytochalasin. *J. Cell Sci.* **72**:327.
7. BRECKHEIMER-BEYRICH, H. 1954. Weitere Erkentnisse über die Wirkung zentrifugaler Kräfte auf das Protoplasma von *Nitella flexilis*. *Ber. Dtsch. Bot. Ges.* **67**:86.
8. CORTI, B. 1774. Osservazioni microscopiche sulla tramella e sulla circulazione del fluido in una pianta aquajuala. Lucca.
9. DONALDSON, I. G. 1972. The estimation of the motive force for protoplasmic streaming in *Nitella*. *Protoplasma.* **74**:329.
10. DONALDSON, I. G. 1972. Cyclic longitudinal fibrillar motion as a basis for steady rotational protoplasmic streaming. *J. Theor. Biol.* **37**:75.
11. DOUGLAS, G. J., and M. E. J. HOLWILL. 1972. Flagella from *Crithidia oncopelti*. *J. Mechanochem. Cell Motility.* **1**:213.
12. EINSTEIN, A. 1905. On the movement of small particles suspended in a stationary liquid demanded by the molecular-kinetic theory of heat. *Ann. d. Phys.* **17**:549. *In* Albert Einstein. Investigations on the theory of the brownian movement. R. Fürth, editor. 1956. Dover Publications Inc., New York. 1.
13. FENSOM, D. S. 1972. A theory of translocation in phloem of *Heracleum* by contractile protein microfibrillar material. *Can. J. Bot.* **50**:479.
14. GRAY, J. 1928. Ciliary Movement. Cambridge University Press, New York.
15. GRAY, J., and G. J. HANCOCK. 1955. The propulsion of sea-urchin spermatozoa. *J. Exp. Biol.* **32**:802.
16. HANCOCK, G. J. 1953. Self-propulsion of microscopic organisms through liquids. *Proc. R. Soc. Ser. A.* **217**:96.
17. HAYASHI, T. 1960. Experimental studies on protoplasmic streaming in *Characeae*. *Sci. Pap. Coll. Gen. Edu. Univ. Tokyo.* **10**:245.
18. HAYASHI, T. 1964. Role of the cortical gel layer in cytoplasmic streaming. *In* Primitive Motile Systems in Cell Biology. R. D. Allen and N. Kamiya, editors. Academic Press, Inc., New York. 19.
19. HEJNOWICZ, Z. 1970. Propagated disturbances of

transverse potential gradient in intracellular fibrils as the source of motive forces for longitudinal transport in cells. *Protoplasma.* **71**:343.

20. HOLWILL, M. E. J., and M. A. SLEIGH. 1967. Propulsion by hispid flagella. *J. Exp. Biol.* **47**:267.
21. HUXLEY, H. E. 1969. The mechanism of muscular contraction. *Science (Wash. D. C.).* **164**:1356.
22. JAROSCH, R. 1955. Untersuchungen Uber Plasmaströmung. Doctoral Thesis. University of Vienna, Austria.
23. JAROSCH, R. 1958. Die Protoplasmafibrillen der Characeen. *Protoplasma.* **50**:93.
24. JAROSCH, R. 1960. Die Dynamik im Characeen-Protoplasma. *Phyton Ann. Rei. Bot.* **15**:43.
25. JAROSCH, R. 1963. Grundlagen einer Schrauben-Mechanik des Protoplasmas. *Protoplasma.* **57**:448.
26. JAROSCH, R. 1964. Screw-mechanical basis of protoplasmic movement. *In* Primitive Motile Systems in Cell Biology. R. D. Allen and N. Kamiya, editors. Academic Press, Inc., New York. 599.
27. KAMITSUBO, E. 1966. Motile protoplasmic fibrils in cells of *Characeae.* I. Movement of fibrillar loops. *Proc. Jap. Acad.* **42**:507.
28. KAMITSUBO, E. 1966. Motile protoplasmic fibrils in cells of *Characeae.* II. Linear fibrillar structures and its bearing on protoplasmic streaming. *Proc. Jap. Acad.* **42**:640.
29. KAMITSUBO, E. 1972. Motile protoplasmic fibrils in cells of the *Characeae. Protoplasma.* **74**:53.
30. KAMITSUBO, E. 1972. A "window technique" for detailed observation of characean cytoplasmic streaming. *Exp. Cell Res.* **74**:613.
31. KAMITSUBO, E. 1972. Destruction and restoration of the protoplasmic fibrillar structure responsible for streaming in the *Nitella* cell. Symposia on Cell Biology. Okayama, Japan. **23**:123.
32. KAMIYA, N. 1959. Protoplasmic streaming. *Protoplasmatologia.* **8**(3a):1.
33. KAMIYA, N. 1962. Protoplasmic streaming. *Handb. Pflanzenphysiol.* XVII(2):979.
34. KAMIYA, N., and K. KURODA. 1956. Velocity distribution of the protoplasmic streaming in *Nitella* cells. *Bot. Mag. (Tokyo).* **69**:544.
35. KAMIYA, N., and K. KURODA. 1958. Measurement of the motive force of the protoplasmic rotation in *Nitella. Protoplasma.* **50**:144.
36. KAMIYA, N., and K. KURODA. 1964. Rotational protoplasmic streaming in *Nitella* and some physical properties of the endoplasm. *In* Symposium on Biorheology. A. L. Copley, editor. Interscience Publishers, Inc., John Wiley & Sons, Inc., New York. 157.
37. KERSEY, Y. 1972. Observations on the streaming cytoplasm and motion in cytoplasts of characean algae: role of microfilaments. Doctoral Thesis. University of California, Irvine, Calif.
38. KURODA, K. 1964. Behavior of naked cytoplasmic drops isolated from plant cells. *In* Primitive Motile Systems in Cell Biology. R. D. Allen and N. Kamiya, editors. Academic Press, Inc., New York. 31.
39. LAFOUNTAIN, J. R., F. A. MUCKENTHALER, and R. D. ALLEN. 1968. Argon ion laser as a source for physical microscopy. *Biophys. Soc. Annu. Meet. Abstr.* **8**:A-159.
40. MACROBBIE, E. A. C. 1971. Phloem translocation. Facts and mechanisms: a comparative survey. *Biol. Rev. (Camb.).* **46**:429.
41. NAGAI, R., and L. I. REBHUN. 1966. Cytoplasmic microfilaments in streaming *Nitella* cells. *J. Ultrastruct. Res.* **14**:571.
42. O'BRIEN, T. P., and K. V. THIMANN. 1966. Intracellular fibers in oat coleoptile cells and their possible significance in cytoplasmic streaming. *Proc. Natl. Acad. Sci. U. S. A.* **56**:888.
43. PALEVITZ, B. A., J. F. ASH, and P. K. HEPLER. 1974. Actin in the green alga, *Nitella. Proc. Natl. Acad. Sci. U. S. A.* **71**:363.
44. PARTHASARATHY, M. V., and K. MÜHLETHALER. 1971. Cytoplasmic filaments in plant cells. *J. Ultrastruct. Res.* **38**:46.
45. PEKAREK, J. 1933. Absolute Viskositätsmessungen mit hilfe der Brownschen Molekularbewegung IV. *Protoplasma.* **17**:1.
46. PICKETT-HEAPS, J. D. 1967. Ultrastructure and differentiation in *Chara* sp. *Aust. J. Biol. Sci.* **20**:539.
47. REBHUN, L. I. 1959. Studies of early cleavage in the surf clam, *Spisula solidissima* using methylene blue and toluidene blue as vital stains. *Biol. Bull. (Woods Hole).* **117**:518.
48. REBHUN, L. I. 1967. Structural aspects of saltatory particle movement. *J. Gen. Physiol.* **50**(6,Pt.2):223.
49. REBHUN, L. I. 1972. Polarized intracellular transport, saltatory movements and cytoplasmic streaming. *Int. Rev. Cytol.* **32**:93.
50. SABNIS, D. D., and W. P. JACOBS. 1967. Cytoplasmic streaming and microtubules in the coenocytic marine algae, *Caulerpa prolifera. J. Cell Sci.* **2**:465.
51. SANGER, J. W., and R. B. HILL. 1972. Disposition of thick and thin filaments in smooth muscle as a function of length and tension. *J. Cell Biol.* **55**(2,-Pt.2):225 a. (Abstr.).
52. SATIR, P. 1968. Studies on cilia. III. Further studies on the cilium tip and a "sliding filament" model of ciliary motility. *J. Cell Biol.* **39**:77.
53. SIBAOKA, T., and K. ODA. 1956. Shock stoppage of the protoplasmic streaming in relation to the action potential in *Chara. Sci. Rep. Tohoku Univ. Fourth Ser. (Biol.).* **22**:157.
54. SUMMERS, K. E., and I. R. GIBBONS. 1971. Adenosine triphosphate-involved sliding of tubules in trypsin-treated flagella of sea-urchin sperm. *Proc. Natl. Acad. Sci. U. S. A.* **68**:3092.

55. TAYLOR, D. L., J. S. CONDEELIS, P. L. MOORE, and R. D. ALLEN. 1973. The contractile basis of amoeboid movement. I. The chemical control of motility in isolated cytoplasm. *J. Cell Biol.* **59**:378.
56. TAYLOR, E. W. 1964. Brownian and saltatory movements of cytoplasmic granules and the movement of anaphase chromosomes. *In* Symposium on Biorheology. A. L. Copley, editor. Interscience Publishers, Inc., John Wiley & Sons, Inc., New York. 175.
57. TAYLOR, G. I. 1951. Analysis of the swimming of microscopic organisms. *Proc. R. Soc. Ser. A.* **209**:447.
58. TAYLOR, G. I. 1952. The action of waving cylindrical tails in propelling microscopic organisms. *Proc. R. Soc. Ser. A.* **211**:225.
59. TAZAWA, M. 1968. Motive force of the cytoplasmic streaming in *Nitella. Protoplasma.* **65**:207.
60. THORNBURG, W. 1967. Mechanisms of biological motility. *In* Theoretical and Experimental Biophysics. A. Cole, editor. Marcel Dekker, Inc., New York. 77.
61. VOROB'EVA, J. A., and B. F. POGLAZOV. 1963. Isolation of contractile protein from the alga *Nitella flexilis. Biofizika.* **8**:474.
62. WESSELS, N. K., B. S. SPOONER, J. F. ASH, M. O. L. BRADLEY, M. A. LUDUENA, E. L. TAYLOR, J. T. WRENN, and K. M. YAMADA. 1971. Microfilaments in cellular and developmental processes. *Science (Wash. D. C.).***171**:135.
63. WILLIAMS, N. S. 1970. Light effects on protoplasmic streaming in *Acetabularia crenulata.* Master's Thesis. University of Maryland, College Park, Md.
64. WILLIAMSON, R. E. 1972. A light-microscope study of the action of cytochalasin B on the cells and isolated cytoplasm of the *Characeae. J. Cell Sci.* **10**:811.
65. YOTSUYANAGI, Y. 1953. Recherches sur les phénomènes moteurs dans les fragments de protoplasme isolés. I. Movement rotatoire et le processus de son apparition. *Cytologica (Tokyo).* **18**:146.
66. YOTSUYANAGI, Y. 1953. Recherches sur les phénomènes moteurs dans les fragments de protoplasme isolés. II. Divers mouvements determinés par la condition de milieu. *Cytologia (Tokyo).* **18**:202.